Available online at www.sciencedirect.com
SCIENCE DIRECT®
Cryobiology 48 (2004) 157–178
CRYOBIOLOGY
www.elsevier.com/locate/ycryo

Cryopreservation of organs by vitrification: perspectives and recent advances☆

Gregory M. Fahy,* Brian Wowk, Jun Wu, John Phan, Chris Rasch, Alice Chang, and Eric Zendejas

21st Century Medicine, Inc., 10844 Edison Court, Rancho Cucamonga, CA 91730, USA

Received 29 September 2003; accepted 18 February 2004

Abstract

The cryopreservation of organs became an active area of research in the 1950s as a result of the rediscovery of the cryoprotective properties of glycerol by Polge, Smith, and Parkes in 1949. Over the ensuing four decades of research in this area, the advantages of vitrification, or ice-free cryopreservation, have become apparent. To date, experimental attempts to apply vitrification methods to vascularized whole organs have been confined almost entirely to the rabbit kidney. Using techniques available as of 1997, it was possible to vitrify blood vessels and smaller systems with reasonable success, but not whole organs. Beginning in 1998, a series of novel advances involving the control of cryoprotectant toxicity, nucleation, crystal growth, and chilling injury began to provide the tools needed to achieve success. Based on these new findings, we were first able to show that an 8.4 M solution (VMP) designed to prevent chilling injury at −22 °C was entirely non-toxic to rabbit kidneys when perfused at −3 °C and permitted perfusion–cooling to −22 °C with only mild additional damage. We next investigated the ability of the kidney to tolerate a 9.3 M solution known as M22, which does not devitrify when warmed from below −150 °C at 1 °C/min. When M22 was added and removed at −22 °C, it was uniformly fatal, but when it was perfused for 25 min at −22 °C and washed out simultaneously with warming, postoperative renal function recovered fully. When kidneys loaded with M22 at −22 °C were further cooled to an average intrarenal temperature of about −45 °C (about halfway through the putative temperature zone of increasing vulnerability to chilling injury), all kidneys supported life after transplantation and returned creatinine values to baseline, though after a higher transient creatinine peak. However, medullary, papillary, and pelvic biopsies taken from kidneys perfused with M22 for 25 min at −22 °C were found to devitrify when vitrified and rewarmed at 20 °C/min in a differential scanning calorimeter. It remains to be determined whether this devitrification is seriously damaging and whether it can be suppressed by improving cryoprotectant distribution to more weakly perfused regions of the kidney or by rewarming at higher rates. In conclusion, although the goal of organ vitrification remains elusive, the prospects for success have never been more promising.
© 2004 Elsevier Inc. All rights reserved.

Keywords: Cryoprotective agents; Isolated perfused kidney; Perfusion; Tissue banking; Dimethyl sulfoxide; Formamide; Ethylene glycol; Organ bank; VS55; VS41A; Tonicity; Viability–stability plot; qv^*; Ice blockers; V_{EG}; VM3; LM5; X-1000; Z-1000

☆ This work was funded by 21st Century Medicine, Inc.
* Corresponding author. Fax: 1-909-466-8618.
E-mail address: gfahy@21cm.com (G.M. Fahy).

0011-2240/$ - see front matter © 2004 Elsevier Inc. All rights reserved.
doi:10.1016/j.cryobiol.2004.02.002

One of the greatest challenges in cryobiology is the cryopreservation of entire organs. Although difficult, this goal is important [40,55,57] in part because present limits on human organ storage times after procurement for transplantation substantially reduce the effectiveness and increase the cost of organ replacement [29]. These problems could be eliminated if organs could be banked [16,40,41] and stored for times that are shorter than current organ recipient waiting times. Although organ cryopreservation has usually been conceptualized as a way of facilitating the replacement of vital organs by allografts or xenografts, there is also considerable current interest in using the technique to preserve gonads during chemotherapy and then return them to the donor after the completion of treatment [57]. Indefinite-term cryopreservation is probably also essential for solving the largest problem in transplantation medicine, which is the shortfall in organ availability in relation to the total number of transplants that are needed. To address this need, a multi-billion dollar investment in the field of tissue engineering has been made [37], but this approach will require cryopreservation in order to achieve inventory control and efficient supply chain management of the tissue-engineered products [26].

The pursuit of organ cryopreservation by vitrification has illuminated many basic phenomena in cryobiology [12,14–16,18,38,58,59], led to practical advances in the cryopreservation of simpler systems [18,46,54], and even inspired new lines of research on simpler systems [2]. Similarly, the present detailed progress report describes advances not only in applied organ cryopreservation but also in several fundamental aspects of cryobiology that are germane to specialists in different cryobiological sub-disciplines. To put these advances in context, a brief and necessarily selective historical overview of key issues will be helpful.

Historical perspectives

The potential advantages of vital organ banks have been recognized for several decades [27,41,55]. The rediscovery of the cryoprotective properties of glycerol in 1949 [45] led to an explosion of interest in cryopreservation of cells and tissues [51] and, as early as 1957, to the first attempt to perfuse a mature mammalian organ with a cryoprotectant and preserve it by cooling to −20 °C or below [50]. In these pioneering experiments of Audrey Smith, hamster hearts perfused with 15% glycerol and exposed to −20 °C resumed a rhythmic beat after thawing, but recovery was not obtained after freezing to lower temperatures [52]. Shortly thereafter, however, Smith and J.E. Lovelock were able to show that guinea pig uterine horns frozen to −79 °C in 20% glycerol did regain near-normal contractile ability after thawing [52]. The study of organ freezing thereafter exploded, peaking in the 1960s and 1970s and continuing into the 1980s. Various degrees of success were claimed in most of the published studies, but no report to this day has described better results than those achieved by Smith and Lovelock with the possible exception of the survival of a minority of canine small bowel segments after seven days of storage in liquid nitrogen and subsequent transplantation [21]. Very recent reports have described the ability of one of seven frozen–thawed rat ovaries transplanted using vascular anastomosis to give rise to normal young [57] and some degree of preservation of blood vessels in frozen–thawed sheep ovaries [20], but no laboratory has demonstrated consistent and practical success in the cryopreservation of any organ that depends on immediate vascular integrity for its in vivo functional recovery.

All reported attempts at organ freezing have been plagued by major methodological problems, but this may not be the main explanation for the failures encountered to date. The great majority of these studies have involved attempts to cryopreserve either the kidney or the heart, but present evidence suggests that the formation of any substantial amount of ice in either the kidney or the heart may be intrinsically incompatible with fully satisfactory recovery after thawing. This conclusion emerged in part from careful ultrastructural studies of freeze-substituted tissues [5,23,28,43] and particularly from rigorous functional studies that linked severe damage directly to ice formation per se, as distinguished from the other factors present during freezing and thawing [43,44].

Fortunately, Farrant [19] and Huggins [22], in 1965, both independently envisioned a way toward the cryopreservation of organs that involved strongly suppressing or even totally preventing ice formation even at very low temperatures. Farrant's specific method allowed both adult guinea pig uteri [19], which can be preserved successfully by freezing as discussed above, and frog hearts [47], which cannot survive freezing, to be recovered after cooling to dry ice temperature. In direct pursuit of Farrant's approach, the Mill Hill group in London [40,49] and Adem and Harness [1] built the first equipment capable of perfusing whole organs with cryoprotectant and washing out the cryoprotectant in a controlled and adequately documented manner. Farrant's original method of incrementally adding cryoprotectant and cooling in multiple steps so as to stay close to the ternary phase diagram (melting point curve) for the DMSO–water–NaCl system may be unworkable [30]. Nevertheless, his innovative concept of completely preventing ice formation even at low temperatures combined with the seminal demonstration by Pegg's group that multimolar concentrations of cryoprotectant can be tolerated by whole organs when osmotic damage is limited [25,42] ultimately permitted the advent of current concepts of organ vitrification, or ice-free preservation in the glassy state [8,13,16].

Vitrification currently appears to be the most likely pathway to successful cryopreservation of organs. Much progress toward this goal has been reported, but many formidable problems have also been encountered. The most encouraging initial breakthrough was the ability to perfuse kidneys with an unprecedentedly concentrated (7.5 M) vitrification solution (VS4) at −3 °C with immediate functional recovery [11] and good quality post-transplant life support capability [29]. However, VS4 will only vitrify at 1000 atm of hydrostatic pressure, and increasing pressure in the presence of this solution resulted in no surviving kidneys [34], making it clear that higher concentrations were needed to eliminate the need for high pressure. A version of VS4 that vitrifies at 1 atm (VS41A) was therefore created by increasing all cryoprotectants of VS4 to a total concentration of 8.4 M (or 55% w/v) [12]. However, this solution (also known as VS55 [53,54]) did not permit consistent survival or immediate function of rabbit kidneys even when exposure to this solution was confined to approximately −24 °C [3,32,33]. Even relatively simple rabbit external jugular veins also showed structural [53] and functional [54] changes in comparison to fresh untreated veins after vitrification and rewarming with VS41A.

In addition to the problem of vitrification solution toxicity, another problem for organ vitrification has been injury caused by cooling to subzero temperatures in the absence of ice formation (so-called chilling injury). Directly cooling organs perfused with 7.5–8 M concentrations of the cryoprotectants of VS41A from −3 to −30 °C produced marked injury [33], consistent with earlier observations on kidneys perfused with other cryoprotectants and cooled to higher subzero temperatures [24,44]. This phenomenon is also readily detectable in renal cortical slices [12]. Although it was found that this injury could be avoided by cooling to about −24 °C in the presence of only 6.1 M cryoprotectant [12,31], this approach was later found to result in so much more chilling injury when the temperature was further reduced as to be even worse than simple cooling in VS41A from 0 °C [30].

A final outstanding problem for organ vitrification has been the difficulty of rewarming vitrified organs rapidly enough to outrun devitrification. The critical warming rate for VS41A, for example, has been estimated at between 40 and 270 °C/min, depending on the assumption used to define the critical warming rate [38]. Rates on this order cannot be attained by simple conduction and will require sophisticated electromagnetic rewarming methods (see Wusteman et al. in the present proceedings), assuming such methods are both physically and biologically feasible.

Recent advances in the fundamental cryobiology of organ vitrification

Improved vitrification solutions

Recently, a substantial advance in the control of cryoprotectant toxicity was described that was

based in part on choosing weaker glass-forming agents over stronger ones [18]. In addition to improving the compositional parameter called qv^* (defined [18] as M_W/M_{PG}, where M_W is the molarity of water in the solution and M_{PG} is the molarity of water-bonding groups in the solution at the concentration needed to vitrify), which seems to link water hydrogen bonding intensity to solution toxicity [18], the specific avoidance of 1,2-propanediol may also be important for preventing toxicity to the vascular endothelium [24]. A further advance was the finding that it was possible to improve the amorphous state stability of these low-toxicity vitrification solutions by incorporating especially effective extracellular polymers, particularly polyvinylpyrrolidone of unusually low relative molecular mass ($M_r \sim 5000$ Da, or PVP K12 [17]), PEG 1000 [17], and two complementary [58] antinucleating agents [58,59] or "ice blockers." The combination of lower toxicity and higher stability has recently allowed the usual goal of attaining a concentration that is just sufficient to permit vitrification (C_V) to be transcended. As explained in Fig. 1, it is now possible to contemplate concentrations that are sufficient to virtually or even entirely prevent devitrification even during relatively slow rewarming.

Fig. 1 shows a supplemented phase diagram for glycerol in water that depicts the concentration dependence of the melting point of the solution (T_m), the homogeneous nucleation temperature (T_h), the temperature at which the solution devitrifies (freezes) upon rewarming at a given warming rate (T_d), and the glass transition temperature (T_g). The concentration needed to vitrify (C_V) is determined, at slow cooling rates (~10 °C/min), by the intersection between the T_h curve and T_g [16] (marked by the circled V). However, at this concentration T_d is well below T_m. Increasing the warming rate raises T_d and reduces the magnitude of devitrification, but very rapid warming rates are typically needed to fully suppress ice formation during rewarming [4,7]. Traditionally, cryobiologists have attempted to use solutions even less concentrated than C_V in order to avoid toxicity. While practical for smaller systems, this approach is untenable for an organ, which may be impossible to rewarm uniformly and safely even at the rate

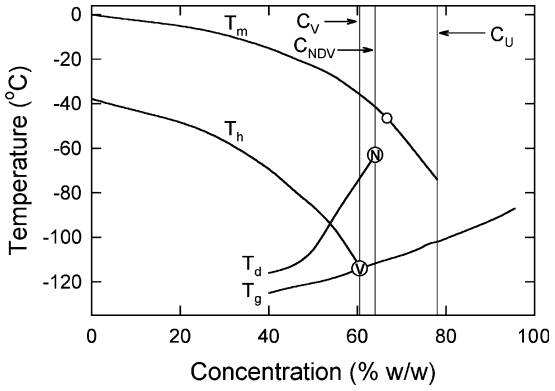

Fig. 1. Supplemented phase diagram for glycerol in water [36,48] showing the relationships between T_m, T_h, T_d, T_g, C_V, C_{NDV}, and C_U (representing, respectively, the temperatures of melting, homogeneous nucleation, devitrification, and the glass transition, the concentration need to vitrify (C_V), the concentration for which no devitrification is observed on slow warming (C_{NDV}), and the maximum concentration that can be achieved as a result of ice formation (C_U, or the concentration at which water becomes unfreezable during freeze-concentration).) C_V is the lowest concentration that remains visibly ice-free on slow cooling and has been found [16] to correspond to the concentration present at the intersection between the T_h and the T_g curves (marked by the circled V). C_{NDV} is defined as the lowest concentration for which the T_d curve vanishes (at the point marked by the circled N). C_{NDV} and the extension of the T_d curve between C_V and C_{NDV} for this system are estimated. The open circle on the T_m curve shows the position of the binary eutectic for glycerol and water, which usually does not crystallize. For further discussion, see text.

required to suppress devitrification at C_V, let alone at the far higher rates required at concentrations lower than C_V. However, T_d also rises rapidly with concentration above C_V, and modest elevations of concentration above C_V can make devitrification undetectable at some temperature below T_m [36] (circled N). It is noteworthy that the concentration at which the T_d curve vanishes (C_{NDV}, for concentration producing no devitrification) is considerably below [36] C_U (the "unfreezable concentration"), at which ice formation ceases during the freezing of nucleated samples [35,36]. Since crystallization is clearly both detectable and possible between C_{NDV} and C_U, the end of the T_d curve, particularly when the warming rate is low, implies the complete suppression of nucleation. In the absence of nucleation, even large vitrified organs should, in

principle, be safe from devitrification during slow rewarming by simple conduction. Such a prospect has been out of the question due to the overwhelming toxicity of cryoprotectants even at C_V [3], but the advances just described have allowed this issue to be revisited.

As concentration is increased to approach the true C_{NDV} (point of complete suppression of nucleation) of the system, the critical warming rate needed to adequately or fully suppress detectable crystallization, v_{WCR}, approaches zero. Therefore, we used v_{WCR} as a practical measure of proximity to C_{NDV}. Fig. 2 plots the recovery of functionality of rabbit renal cortical slices (based on the ability to restore a physiological K^+/Na^+ ratio after cryoprotectant washout) against the v_{WCR} of the solution to which they were exposed (Table 1), a representation we call a viability–stability plot. Here v_{WCR} is defined as the warming rate required to confine crystallization to approximately 0.2% of the mass of an average sample based on triplicate differential scanning calorimetric (DSC) measurements, a

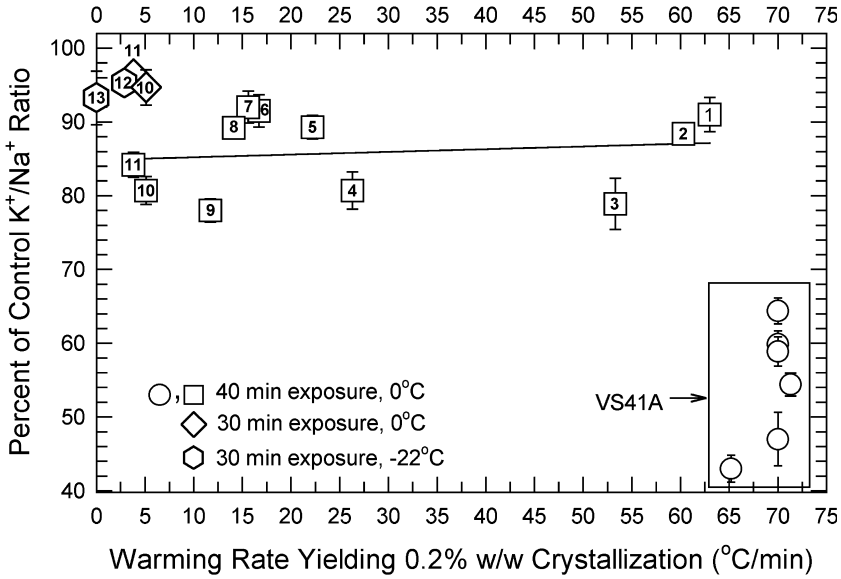

Fig. 2. "Viability–stability plot" for rabbit renal cortical slices exposed to 14 different vitrification solutions. In this type of plot, the biological recovery of the system after exposure to a vitrification solution is plotted against the critical warming rate of the tested vitrification solution. In this figure, the critical warming rate was defined as the rate that was sufficient to suppress crystallization of all but 0.2% of the test solution mass, as measured by the enthalpy of melting. The numbers inside the plotted symbols refer to the numbers of the corresponding solutions listed in Table 1, except that point 13 refers to data obtained for the M22 formula of Table 2. Viability is assessed using the steady-state K^+/Na^+ ratio achieved by the slices after cryoprotectant washout and 90 min of incubation at 25 °C followed by washout of most extracellular cations with isotonic mannitol [5,6,14]. The results shown (means ± 1 SEM) represent data from a large number of individual experiments, each data point representing generally about 12 individual K^+/Na^+ ratios. In part because absolute control K^+/Na^+ ratios vary from experiment to experiment, all treatment results are normalized to untreated control K^+/Na^+ ratios. Results for slices exposed to VS41A are represented by the circles within the box at the right of the graph. Stability variations for VS41A arise from testing in different carrier solutions (order of increasing critical warming rate: EC < RPS-2 < LM5). Results for slices exposed to more recently developed solutions are depicted by squares, diamonds, and hexagons. Circles and squares refer to exposure to full-strength cryoprotectant for 40 min at 0 °C, whereas diamonds show the effects of 30 min at 0 °C and hexagons the effect of 30 min at −22 °C. Most cryoprotectants were introduced (1/8, 1/4, 1/2, and 100% of full-strength, with 20 min at each loading step and 30–40 min at full-strength cryoprotectant) and removed (20 min steps of 1/2, 3/8, 1/4, 1/8, 1/16, and 0% of full-strength cryoprotectant all in the presence of 300 mM mannitol, followed by transfer to carrier solution for at least 20 min before viability testing) using our standard method at 0 °C, with the following exceptions. For 1.5E and M22 exposure (points 12 and 13, respectively), slices were first exposed to VMP (see Table 3 legend for composition) at 0 °C for 20 min according to the above schedule and then transferred to M22 or 1.5E at −22 °C for 30 min, after which they were transferred to half-strength VMP plus 300 mM mannitol at 0 °C to commence washout according to the above schedule. Exposure to 1.5× (point 10) was similar but at 0 °C.

Table 1
Some biologically acceptable, highly stable vitrification solutions[a]

Point	Name	v_{WCR}	D	F	E	A	PK30	P5	X	Z	Carrier	% w/v
1	V_{EG} – 4%D(1)F + 7PK30	63	21.671	12.492	16.837	0	7	0	0	0	RPS-2	58
2	V_{EG} + 1%X	60.3	24.208	13.955	16.837	0	0	0	1	0	LM5	56
3	V_{EG} + 2%D	53.3	24.208	13.955	16.837	0	0	0	0	0	RPS-T	57
4	$E[D(.7)F]_{38.16}$ + 6P5	26.3	20.926	17.234	16.840	0	0	6	0	0	GHP-2	61
5	52% V_{EG}S + 6P5 + .5X + .5Z	22.2	22.887	13.194	15.919	0	0	6	0.5	0.5	LM5	59
6	52% V_{EG}S + 6P5 + 1%X	16.7	22.887	13.194	15.919	0	0	6	1	0	RPS-2	59
7	50% V_{EG}S + 8P5 + 1%X	15.6	22.007	12.686	15.307	0	0	8	1	0	RPS-2	59
8	V_{EG} – 4%D(1)F + 7P5 + .5 + .5	14.1	21.671	12.492	16.837	0	0	7	0.5	0.5	LM5	59
9	$E[D(.7)F]_{38.16}$ + 6P5 + .5 + .5	11.7	20.926	17.234	16.840	0	0	6	0.5	0.5	LM5	62
10	V_{EG} – 3%D(1)F + 7A + 1X + 4Z	5.1	22.305	12.858	16.837	7	0	0	1	4	LM5	64
11	V_{EG} – 3%D(1)F + 7P5 + 1 + 1	3.8	22.305	12.858	16.837	0	0	7	1	1	LM5	61
12	V_{EG} – 3%D(1)F + 7E + 1X + 4Z	2.9	22.305	12.858	23.837	0	0	0	1	4	LM5	64

[a] Solution numbers refer to points in Fig. 2. v_{WCR} is the warming rate required to suppress ice formation to 0.667 J/100 g, which is equivalent to the amount of heat that would be produced by the crystallization of 0.2 g of water per 100 g of solution at 0 °C. v_{WCR} was measured after cooling to −150 °C at 100 °C/min. Cryoprotectant concentrations are given in % w/v (g/dl) units. *Abbreviations:* D, dimethyl sulfoxide; F, formamide; E, ethylene glycol; A, acetol; PK30, PVP K30, of M_r 40,000 Da; P5, PVP K12, of M_r 5000 Da; X, the commercially available Supercool X-1000 ice blocker; Z, the commercially available Supercool Z-1000 ice blocker; (1) and (.7) refer to the molar ratio of dimethyl sulfoxide to formamide in the solution; V_{EG}, a cryoprotectant solution described elsewhere [18] and recapitulated for point 2; V_{EG}S, "V_{EG} Solutes," which refers to the total amount of the sum of the D, F, and E components of V_{EG} (in the proportions found in V_{EG}); the carrier solutions RPS-2, RPS-T, and GHP-2 are described elsewhere [9,17]. The LM5 carrier solution [9] consists of 90 mM glucose, 45 mM mannitol, 45 mM lactose, 28.2 mM KCl, 7.2 mM K_2HPO_4, 5 mM reduced glutathione, 1 mM adenine HCl, 10 mM $NaHCO_3$, and, when cryoprotectant is absent, 1 mM $CaCl_2$ and 2 mM $MgCl_2$. Solution 10 is also known as "1.5×." Solution 11 is also known as VM3. Solution 12 is also known as 1.5E.

standard that exceeds the criterion suggested by Boutron and Mehl [4] of 0.5% crystallization. Data for exposure to VS41A are included as a point of reference. As can be seen, by judicious selection of compositional factors and exposure conditions, it is possible to travel closer and closer to, and perhaps even to literally reach, C_{NDV} (critical warming rate, 0 °C/min) while retaining high functional viability. For example, adding 0.5% w/v of each of polyvinyl alcohol and polyglycerol (the two antinucleators or "ice blockers" referred to above) and changing the carrier solution from a high glucose to a lower glucose carrier known as LM5 (see Table 1) cut v_{WCR} from about 26 °C/min to about 12 °C/min (point 9 vs. point 4), more than a 2-fold gain, with no penalty in toxicity. The same maneuver plus the replacement of PVP K30 with PVP K12 lowered v_{WCR} from 63 to 14 °C/min (point 8 vs. point 1), more than a 4-fold improvement. Elevating the ice blockers by another 0.5% w/v each and increasing permeating cryoprotectant level by 1% w/v (point 11 vs. point 8) yielded an additional 3.7-fold gain with, again, no reduction in functional recovery. Overall, compared to VS41A, the use of ice blockers, PVP K12, and LM5 in combination with permeating cryoprotectant mixtures based on the combination of dimethyl sulfoxide, formamide, and ethylene glycol [18] permits approximately a 20-fold improvement in v_{WCR} with a simultaneous improvement in K^+/Na^+ ratio from about 55% of control to about 85% of control after 40 min of exposure at 0 °C (Fig. 2, squares vs. circles), and with little trend toward higher toxicity as C_{NDV} is approached (see linear regression line through the numbered points). The formula known as VM3 [18] yielded about an average K^+/Na^+ result at 40 min of exposure (square point number 11), but reducing exposure by just 10 min resulted in a ratio approaching that of untreated controls (diamond-shaped point number 11). Similarly, another variant (square point 10, a solution also known as "1.5×") permitted only slightly over 80% recovery relative to controls at 40 min of exposure at 0 °C, but at 30 min of exposure it permitted recovery of $94.7 \pm 2.4\%$ of untreated control K^+/Na^+ (dia-

mond-shaped point number 10). By additionally reducing the temperature of exposure from 0 to −22 °C, a related solution (point 12) containing extra ethylene glycol in place of the acetol of 1.5× also attained an excellent K^+/Na^+ ratio (95.3 ± 1.25% of untreated control) despite a v_{WCR} of only 2.9 °C/min. Finally, exposure at −22 °C for 30 min even allowed good recovery after exposure to one solution (point 13) whose v_{WCR} approaches or equals zero. Warming this solution from below its T_g at 1 °C/min (the lower warming rate limit of our differential scanning calorimeter) failed to reveal any melting endotherm, and numerous efforts to freeze this solution using various cooling and annealing protocols have been unsuccessful. This solution (Table 2) was named M22 because it is intended to be brought into contact with living systems at about −22 °C. The potential application of M22 to the vitrification of whole kidneys is considered in detail below.

Table 2
Properties of M22

Component	Concentration or property
Dimethyl sulfoxide	2.855 M (22.305% w/v)
Formamide	2.855 M (12.858% w/v)
Ethylene glycol	2.713 M (16.837% w/v)
N-Methylformamide	0.508 M (3% w/v)
3-Methoxy,1,2-propanediol	0.377 M (4% w/v)
PVP K12	2.8% w/v (∼0.0056 M)
PVA[a]	1% w/v[b] (∼0.005 M)
PGL[a]	2% w/v[b] (∼0.0267 M)
5× LM5[c]	20 ml/dl
Total cryoprotectant concentration	9.345 M (64.8% w/v)
pH	8.0
Nominal tonicity	1.5 times isotonic
Melting point[d]	∼−54.9 °C (estimated)
Critical warming rate	<1 °C/min

[a] PVA (“Supercool X-1000”) and PGL (“Supercool Z-1000”) are commercially available ice blockers obtainable from 21st Century Medicine, Inc. and consist of a polyvinylalcohol–polyvinylacetate copolymer and polyglycerol, respectively.

[b] Final polymer concentrations.

[c] 1× LM5 (see Table 1 for formula) contains 1 mM $CaCl_2$ and 2 mM $MgCl_2$, but these are omitted from the 5× LM5 to avoid the formation of precipitates. “5× LM5” refers to a 5-fold increase in the molar concentrations of the components of LM5.

[d] This solution could not be frozen and therefore a theoretical melting point could only be obtained by extrapolation of data for 94% v/v and 97% v/v of full-strength M22 (see Fig. 15 for this extrapolation.)

Suppressing chilling injury

The problem of chilling injury in renal cortical tissue is illustrated in Fig. 3. As previously reported [7], vitrification of renal cortex typically results in about a 50% loss of tissue function (upper black bar) compared to the function attained after vitrification solution exposure without vitrification (upper white bar), and this injury is seen whether the cooling rate is rapid or slow [7,12]. Fig. 3 indicates that although the newer vitrification solutions can greatly reduce toxicity prior to vitrification (lower two white bars), vitrification and rewarming (lower two black bars) still

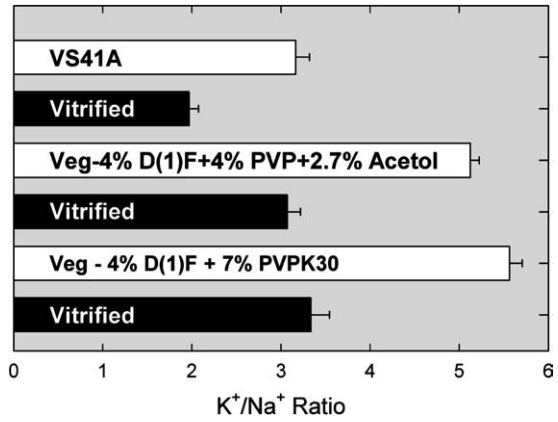

Fig. 3. Failure of the new cryoprotectant formulas to prevent chilling injury upon vitrification. When rabbit renal cortical slices were placed into two typical V_{EG}-based vitrification solutions (V_{EG} is defined in the second entry of Table 1), much less toxicity was apparent than when slices were placed into the older-generation VS41A vitrification solution (compare open bars). Nevertheless, after slices were vitrified (black bars), a similar proportional loss of viability was experienced with all solutions (compare relative lengths of open and corresponding black bars) even though slices vitrified with the new solutions showed recoveries (lower two black bars) similar to the recovery obtained after VS41A treatment in the absence of vitrification (top open bar). “D(1)F” refers to dimethyl sulfoxide and formamide in a 1:1 mole ratio, and “V_{eg}” refers to V_{EG}. “PVP” and “PVPK30” refer to polyvinylpyrrolidone with a mean mass of about 40,000 Da. All percents refer to concentrations in % w/v units. Cryoprotectants were added and removed at 0 °C as described in the legend of Fig. 2. Means ± 1 SEM.

reduce the pre-cooling tissue function by about 50%. Although the injury shown after vitrification in this figure is presumed to be caused by chilling injury, another possibility is that it is the result of nucleation and crystal growth during cooling and warming. The latter possibility, however, is unlikely based on the data of Fig. 4, which maps the magnitude of renal cortical cooling injury in VM3 against the lowest temperature to which the tissue was slowly cooled before rapid rewarming. The results show that chilling injury steadily increases in this system between 0 and about −85 °C, but does not increase further upon cooling below this range. Given that nucleation is more likely below −85 °C than above this temperature [38], the temperature dependence of cooling injury is the opposite of the temperature dependence of any injury expected to result from nucleation.

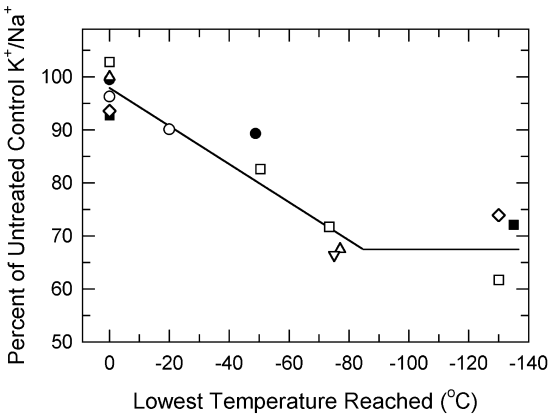

Fig. 4. Chilling injury as a function of temperature during the cooling of rabbit renal cortical slices after treatment with VM3. Each symbol refers to an independent experiment. Each point reflects two replicate groups of six slices per group cooled slowly in 3–80 ml of VM3 with individual thermocouples to allow cooling to be monitored and interrupted at desired temperatures. Cooling profiles were curvilinear and were typically completed in 10–25 min; warming was rapid and typically was completed in 1–5 min. No effect of sample volume, cooling rate, or warming rate was apparent. Note lack of damage caused by VM3 exposure only, without cooling to subzero temperatures (93–103% of untreated control K^+/Na^+ ratio for points plotted at 0 °C). Upon reaching the temperatures shown, slices were immediately rewarmed and transferred to washout solution (half-strength VM3 plus 300 mM mannitol) at 0 °C. Standard errors, omitted for clarity, were typical of errors shown in Fig. 5. The line extending from 0 to ∼−85 °C is a least squares linear regression through the data for slices cooled to above −80 °C.

An effective remedy for the problem of chilling injury was discovered as a serendipitous result of experiments intended to simulate freezing injury [10]. When freezing takes place, the concentrations of cryoprotectant and carrier solution increase simultaneously with temperature reduction, whereas vitrification is often carried out in an isotonic carrier solution. We found that isothermal elevation and reduction of carrier solution concentration in proportion to the elevation and reduction in cryoprotectant concentration was innocuous for kidney slices [10]. The next step was to cool slices to −20 °C in solutions of varying carrier solution concentration to see what effect the hypertonicity of the carrier might have. Although previous observations suggested that hypertonicity or high cryoprotectant concentration or both are the factors that cause chilling injury in kidney tissue [12,31,32], the experiments shown in Fig. 5 indicate that neither factor is an intrinsic problem and, to the contrary, that hypertonicity within certain limits is actually highly protective.

In the first experiment (Fig. 5A, $1\times \rightarrow 1\times$), slices equilibrated for 20 min in a typical isotonic vitrification solution (for formula, see Fig. 5A) were transferred from this solution at 0 °C (open bar) to the same solution at −20 °C (shaded bar). This control experiment showed that cooling to −20 °C in an isotonic vitrification solution resulted in only slightly over 60% recovery of control K^+/Na^+ ratio. The effect of this procedure was compared to the effect of similar cooling in a vitrification solution (V2X, see Fig. 5 legend) containing a 2× RPS-2 carrier (twice the normal amount of RPS-2 solutes per unit volume). V2X was not only not damaging before cooling (open bar at $2\times \rightarrow 2\times$ in Fig. 5A), but appeared to virtually abolish cooling injury at −20 °C (shaded bar, $2\times \rightarrow 2\times$ group). The $1\times \rightarrow 2\times$ bar represents slices that were equilibrated with a sub-vitrifiable (6.1 M), non-toxic, isotonic cryoprotectant solution (see legend for formula) at 0 °C, and then transferred to V2X at −20 °C. According to previous theory [12,31], the results of the $1\times(0\,^\circ\mathrm{C}) \rightarrow 2\times(-20\,^\circ\mathrm{C})$ treatment should have been superior to the results of the $2\times(0\,^\circ\mathrm{C})$

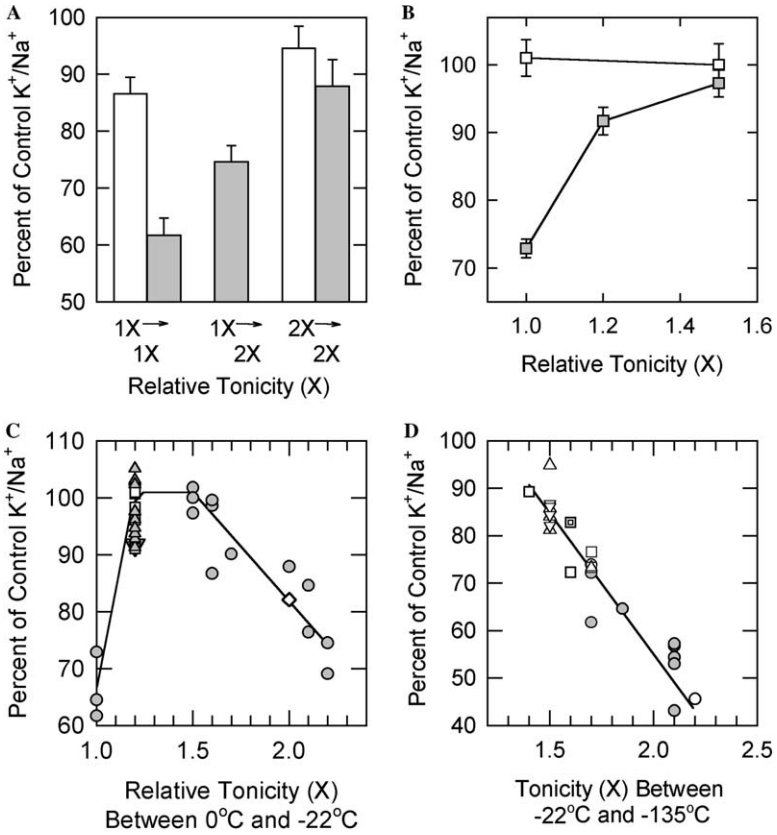

Fig. 5. Hypertonic modification of chilling injury. (A–C) Modification of injury caused by abrupt transfer of slices from solutions at 0 °C to solutions at −20 °C. Cryoprotectant addition and washout was accomplished as described in the legend of Fig. 2, standard method. (A) The effects of three contrasting osmotic treatments on chilling injury. In the $1\times \rightarrow 1\times$ group, slices were treated at 0 °C with a vitrification solution consisting of V_{EG} + 2% w/v dimethyl sulfoxide in an RPS-2 carrier solution (see Table 2 for the formula of V_{EG}). The white bar shows the effect of exposure to this solution at 0 °C and the shaded bar shows the effect of transferring slices to the same solution precooled to −20 °C. After 20 min at −20 °C, washout took place at 0 °C as usual. The $2\times \rightarrow 2\times$ group employed the same procedure but the vitrification solution (V2X) consisted of V_{EG} at 52/55 of its standard concentration in a 2× RPS-2 solution (twice the normal amount of RPS-2 solutes per unit volume). In contrast to the $1\times \rightarrow 1\times$ group, the recovery after cooling (shaded bar) was similar to the recovery after 0 °C exposure (white bar). The $1\times \rightarrow 2\times$ group involved equilibration with 40/55 of full-strength V_{EG} in isotonic RPS-2 at 0 °C followed by transfer to −20 °C V2X (shaded bar). (B) Slices were treated using the same protocol as in (A) but after exposure to V_{EG} minus 3% w/v D(1)F in varying tonicities of LM5 at 0 °C. White boxes: exposed to cryoprotectant and varying LM5 tonicities at 0 °C only; gray boxes: exposed to cryoprotectant and varying LM5 tonicities at 0 °C and then cooled to −20 °C at the same tonicities. (C) Overall results of several chilling injury experiments involving a variety of cryoprotectant solutions and methods of elevating tonicity. Unless otherwise stated, slices were transferred from a given solution at 0 °C to the same solution precooled to −22 °C. Squares at $1.2\times$ = tonicity elevation by 1% addition of each of the two ice blockers (X-1000 and Z-1000). Small triangles at 1.2×: same as squares, but the concentration of cryoprotectant at −22 °C was higher than the concentration at 0 °C though the tonicity of the carrier + polymers was not changed. Large inverted triangle at 1.2×: tonicity elevated by increasing the carrier solution concentration. (D) Hypertonic modulation of chilling injury during cooling to −100 °C and below. Slices treated with a variety of cryoprotectant solutions were cooled in 3–12 ml volumes to −100 °C or below and rewarmed rapidly. Gray circles: cooled through all temperatures at the tonicity plotted. Open points: cooled to −22 °C at a lower tonicity (1.2× or 1.5×) than the tonicity plotted, then switched to the plotted tonicity for further cooling. Each symbol plotted represents generally 12 different individual measurements; error bars, omitted for clarity, were typical of the data shown in Fig. 3 and panels (A)–(C) of this figure. All data are plotted as a percentage of untreated control K^+/Na^+ and therefore show the total effect of both cryoprotectant toxicity and cooling/warming injury. Cooling to −100 to −135 °C was completed within 20–25 min and rewarming was generally completed in 2–4 min.

$\rightarrow 2\times(-20\,^{\circ}C)$ treatment, but in fact, the opposite was found. Further, the fact that the $1\times \rightarrow 2\times$ treatment gave better results than the $1\times \rightarrow 1\times$ treatment shows that renal cortical slices are able to respond favorably to hypertonicity even during the very brief time required for cooling in these experiments.

In the next experiment, the composition of the cryoprotectant formula was held constant and only the concentration of the carrier solution was changed (Fig. 5B). Once again, as the tonicity of the medium increased prior to cooling, chilling injury was progressively suppressed.

A summary of many different experiments involving many different solutions is provided in Fig. 5C. These results confirm that (a) chilling injury can be completely suppressed upon cooling to about −22 °C; (b) the tonicity threshold for this effect is remarkably low (about 1.2× for complete or near-complete suppression of injury); (c) the optimum range of protective tonicities at this temperature is very narrow (about 1.2×–1.5×); and (d) the protective effect is independent of the impermeant solutes used to effect hypertonicity, extracellular polymers producing at least the same effect (see Table 3 for useful osmotic reference data) as an equal osmolality of carrier solution. These results have possible significance for current vitrification protocols for simple systems, which sometimes employ excessively high polymer or other impermeant concentrations that, for systems sensitive to chilling injury, may not be optimally protective.

The abolition of chilling injury at −22 °C leaves unanswered the question of how chilling injury responds to medium tonicity at lower temperatures. As shown in Fig. 5D, continuing cooling to below T_g (i.e., to −125 to −135 °C) produces injury with similar tonicity dependence as the injury observed at −22 °C, although the slope of the line is steeper, presumably due to the accumulation of chilling damage over a larger thermal range. Critically, the same tonicity range that gave essentially no injury at −22 °C appears to be optimal as well at lower temperatures, and by maintaining tonicity within this narrow range injury could routinely be limited to less than a 20% deficit in K^+/Na^+. This is all the more remarkable considering that the data of Fig. 5D also include the contribution of injury from cryoprotectant exposure prior to deep cooling. In the best experiment, the sum total of all injury sustained reduced K^+/Na^+ ratio by only 5% after cooling to −130 °C in a 1.5× solution (solution 10 of Table 1) that was

Table 3
Some useful reference tonicity data

Solution	Osmolality[a]	Tonicity (×)[b]	Polymer osmolality[c]
LM5	283 ± 3 mOsm	1.0	—
LM5 + 1% Z[d]	321 ± 3 mOsm	1.13	Z = 38 mOsm
LM5 + 1% X[e]	291 ± 1 mOsm	1.03	X = 8 mOsm
LM5 + 1% Z + 1% X	330 ± 3 mOsm	1.17	S[f] = 46 mOsm
LM5 + 7% PVP K12	413 ± 2 mOsm	1.46	P[g] = 130 mOsm
LM5 + 7% PVP K12 + 1% Z + 1% X	474 ± 5 mOsm	1.67	S = 191 mOsm
LM5 + 2% Z + 1% X + 2.8% PVP K12	421 ± 3 mOsm	1.49	S = 138 mOsm

[a] Mean ± 1/2 the range of the mean.

[b] Tonicity relative to LM5. Tonicity is defined as π_{Test}/π_{iso}, where π_{Test} is the osmolality of the cryoprotectant-free test solution (made by adding impermeants to the baseline, cryoprotectant-free carrier solution) and π_{iso} is the osmolality of the baseline carrier solution (in this case, the osmolality of LM5, i.e., 283 mOsm). It is assumed that all carrier solution components are impermeant for practical purposes. It is further assumed that the presence of permeating cryoprotectants has no practically relevant effect on the effective tonicity of the solution.

[c] Mean osmolality −283 mOsm.

[d] Z = Supercool Z-1000 (1% refers to 1% w/v of polyglycerol, not 1% of the commercially available stock 40% w/w solution).

[e] X = Supercool X-1000 (1% refers to 1% w/v of polyvinyl alcohol, not 1% of the commercially available stock 20% w/w solution).

[f] S refers to the sum of polymers listed (X + Z or X + Z + P).

[g] P = PVP K12 ($M_r \sim 5000$ Da).

Note. VMP consists of V_{EG} plus 1% w/v Z-1000 (i.e., 1% w/v polyglycerol) and 1% w/v X-1000 (i.e., 1% w/v polyvinyl alcohol), but no PVP K12. Consequently, its nominal tonicity is 1.17 times isotonic (∼1.2×).

introduced at −22 °C following cooling from 0 °C in a 1.2× solution.

In addition to their practical significance for overcoming the barrier of chilling injury that had remained with the use of previous methods [30], these experiments are of basic theoretical importance. They also support the distinction between chilling injury, which in the present experiments is reduced by elevating tonicity, and thermal shock, which is classically exacerbated by elevating tonicity [56]. The current experiments also clearly indicate that the process of passage through the glass transition per se does not produce any specific cellular or chemical injury since cooling to −85 °C (well above T_g) and to −135 °C (well below T_g) gave equivalent results (Fig. 4).

Applying fundamental advances to the vitrification of whole organs

Cooling kidneys to −22 °C

As reported elsewhere [18], our first step in applying the fundamental advances described above to whole rabbit kidneys was to show that perfusion at −3 °C with the new 8.4 M solution known as VMP (see Table 3 legend for formula) was innocuous. VMP was chosen for initial testing based on the results of Fig. 5. We reasoned that to prepare a kidney for cooling to a temperature at which M22 might be introduced, prior introduction of a 1.2× solution at −3 °C would be appropriate in view of the efficacy of cooling from 0 to −22 °C beginning with a 1.2× solution, the hazards of exceeding a tonicity of 1.5×, and the fact that slices can respond to osmotic disequilibria during cooling from 0 to −22 °C (based on Fig. 5A, 1× → 2× treatment). Because the osmotic contributions of 1% polyvinylalcohol–polyvinylacetate copolymer (PVA) and 1% polyglycerol (PGL) sum to about 0.2×, a convenient way of devising a solution for protecting during cooling was to delete the PVP K12 from VM3 (solution 11 of Table 1) and to use the resulting solution (VMP) as the desired 1.2× solution to be used for cooling to −22 °C. Having established the safety of VMP, the next step was to establish methods of actually cooling whole kidneys perfused with VMP to about −22 °C and rewarming them with good results after transplantation.

Cooling kidneys to −22 °C required several different problems to be confronted and solved. The available literature provided no guidance as to whether this degree of cooling and rewarming by continuous vascular perfusion was compatible with subsequent vascular function in vivo or, if potentially compatible, how it should be carried out. We began as previously described [18] by gradually introducing VMP while temperature gradually fell to −3 °C in a computer-operated perfusion machine. However, instead of continuing VMP perfusion for 20 min at 0 °C, we began abruptly cooling the arterial perfusate by a programmed increase in flow of −25 °C coolant over an in-line arterial heat exchanger after just 10 min of exposure to VMP. After 10 min of cooling at the maximum rate we could achieve, the arterial and venous temperatures approached −22 °C.

We tried three different methods for rewarming the kidneys and removing the VMP. In the first, we immediately began perfusing −3 °C, half-strength VMP plus 300 mM mannitol, which resulted in rapid elevation of arterial temperature. This procedure produced no signs of inducing freezing in the kidney or the arterial perfusate during rewarming, and the total time of exposure to VMP was limited to the 20 min shown to be safe at −3 °C before. Nevertheless, three consecutive kidneys treated in this way failed to support life after transplantation (Fig. 6). Suspecting that the cause of the observed injury might be rapid osmotic expansion of brittle tissues near −20 °C as a result of diluting the cryoprotectant prior to the completion of rewarming, we modified the procedure by introducing a 10-min warming step prior to the onset of cryoprotectant washout. Although this exposed the kidney to VMP perfusion for a total of 30 min, all kidneys survived, and post-transplant function was dramatically improved (Fig. 6). Finally, to probe the possibility that some of the injury observed was due either to the longer total exposure period or to cooling at a tonicity that was insufficient for the vascular bed, we shortened the period of VMP perfusion from 10 to 5 min before cooling to −22 °C, thus limiting the total exposure time to

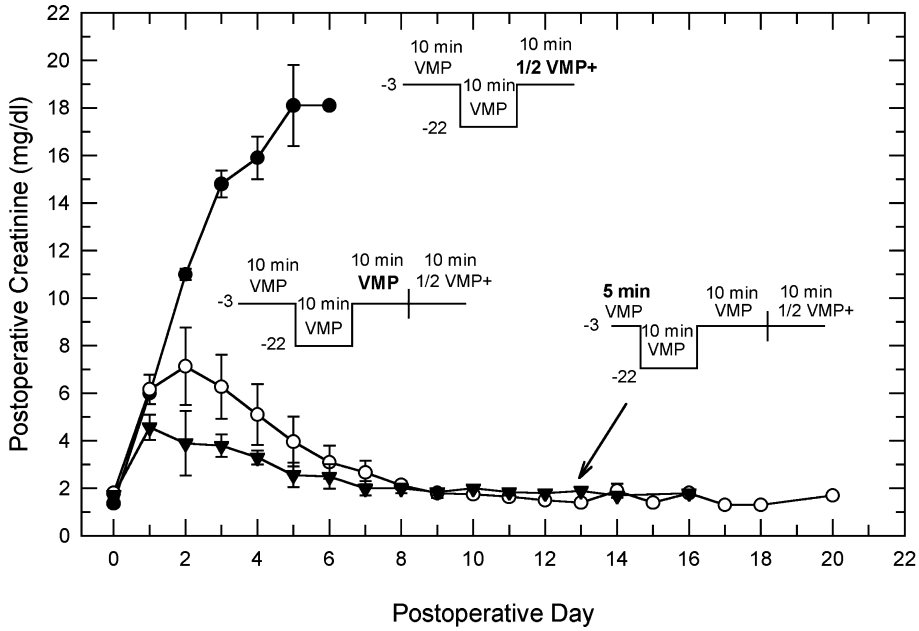

Fig. 6. Effects of three time–concentration–temperature protocols (indicated by protocol schematics) on the quality of recovery of rabbit kidneys (indicated by postoperative serum creatinine levels) perfused with VMP at −22 °C. Each protocol schematic represents the time (horizontal direction) and temperature (vertical direction) of the initial VMP perfusion step at −3 °C, the cooling step involving the perfusion of VMP at temperatures down to −22 °C, and the subsequent warming and dilution steps. The concentration perfused at each step is indicated above the schematic line. Bold text in the protocol schematics indicates key differences between the tested protocols. For discussion, see text. In each case, the preserved kidney served as the sole renal support immediately after transplantation. For each group, $n = 3$. Means ± 1 SEM.

VMP to 25 min and increasing osmotic disequilibrium at the onset of cooling. This change reduced mean peak creatinine values substantially (Fig. 6) and demonstrates that chilling injury can in fact be suppressed almost entirely at ~−22 °C in whole rabbit kidneys using the final method shown in Fig. 7.

Perfusing kidneys with M22

Although VMP can be vitrified, it is much too unstable to be used as a final vitrification solution for kidneys. We chose to explore the possibility of using M22 for the vitrification of kidneys in view of its extraordinary stability and reasonable toxicity at −22 °C (Fig. 2). However, tissue slice experiments suggested that exposure to M22 at −3 °C would produce unacceptable toxicity, unlike exposure to VMP as in the rewarming method shown in Fig. 6. On the other hand, washing out M22 at −22 °C could be even more hazardous than washing out VMP at this temperature. It seemed clear that the ability of kidneys to withstand exposure to M22 would depend critically on the method used to wash it out.

Despite the fatality of transitioning from VMP to half-strength VMP + mannitol at −22 °C (50% reduction in molar concentration), the magnitude of the dilution involved in transitioning from M22 to VMP (~10% reduction in molarity) is much smaller. We therefore first considered that this transition might be tolerable at −22 °C despite the evident hazards of osmotic expansion at this temperature. To test this hypothesis, we cooled two kidneys to −22 °C as per the best protocol of Fig. 6, switched to perfusion with M22 at ~−22 °C for 15 min, and then diluted the M22 at −22 °C by perfusion with VMP before perfusing VMP at −3 °C (see washout protocol in Fig. 8, inset, heavy black line). One of these two kidneys sur-

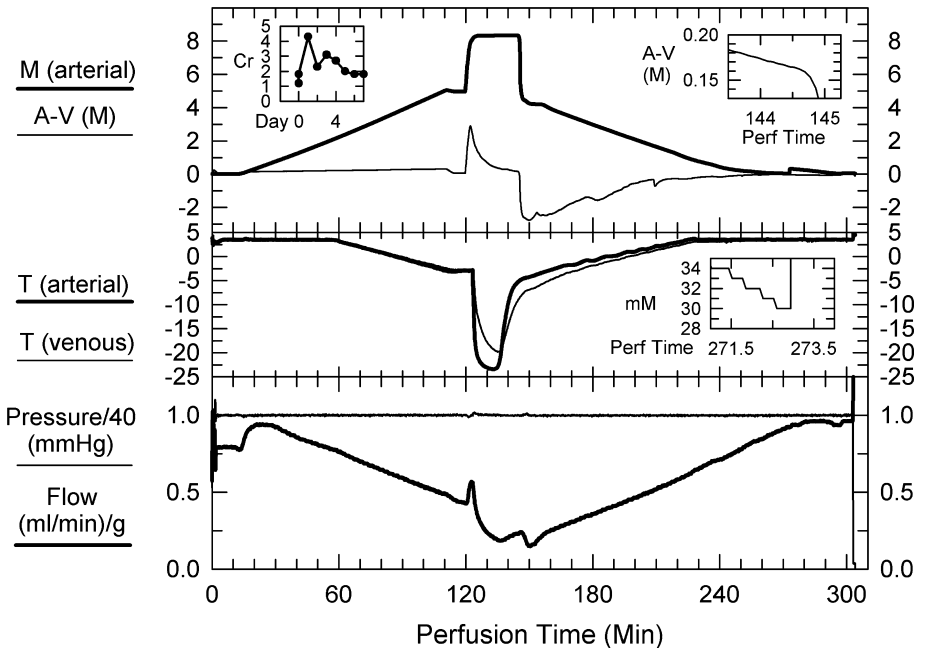

Fig. 7. Details of the best perfusion protocol employed for the successful recovery of VMP-perfused kidneys from −22 °C using automated vascular cooling and warming techniques. The three panels plot perfusion data against a common time base indicated below the lowest panel. The data shown depict a typical perfusion resulting in a peak postoperative creatinine (Cr) level of 4.4 mg/dl (see inset in upper panel; "Day" refers to postoperative day; time zero Cr values represent serum creatinines at nephrectomy and at transplant). Upper panel: arterial molarity (M; heavy line) and the arterio-venous concentration difference across the kidney (A-V) in molar (M) units, as derived from arterial and venous in-line refractometers essentially as in previous perfusion experiments [11,29]. Second inset of upper panel: detail of A-V difference history showing a venous concentration within about 160 mM of the arterial concentration just before cryoprotectant dilution. Middle panel: arterial (heavy line) and venous temperatures (T) in °C as measured using an arterial in-line needle thermocouple and a second fine thermocouple inserted directly in the venous effluent underneath the kidney. Inset: detail taken from the upper panel showing the concentration of cryoprotectants (30 mM) just before switching to a solution containing no cryoprotectant. Upon switching to 0 mM cryoprotectant, the display mode changes to plot the concentration of mannitol being perfused, which starts near 100 mM (off scale in the inset) and gradually declines (data not shown). Lowest panel: arterial perfusion pressure in mmHg and perfusate flow rate (heavy line) in ml/min per gram of post-flush, pre-perfusion kidney weight. Perfusion pressure was divided by 40 to permit it to be plotted on the same scale as the flow rate.

vived, but with a creatinine peak at 18.2 mg/dl (Fig. 8, main panel, heavy black line).

On the assumption that osmotic expansion damage was the main reason for the injury seen in this protocol, the next protocol involved the simultaneous dilution and warming of the kidney by perfusion with −3 °C VMP for 10 min (middle protocol of Fig. 8). Of the six kidneys in this group, all survived, and damage appeared to be generally less than with dilution starting at lower temperatures.

These results suggested that osmotic expansion damage at low temperatures was a more important factor than the toxicity of M22 during brief exposure above −22 °C. We therefore next installed a heating element in the heat exchange path in order to substantially accelerate the rewarming step, and achieved the final warming protocol shown in Fig. 8 (inset, gray line). The result of this treatment was a dramatic improvement in recovery after 15, 20, or even 25 min of previous M22 perfusion, with no increase in injury with increasing M22 perfusion time over this range (data not shown). The overall best 25 min M22 perfusion protocol resulting from these experiments is illustrated in Fig. 9.

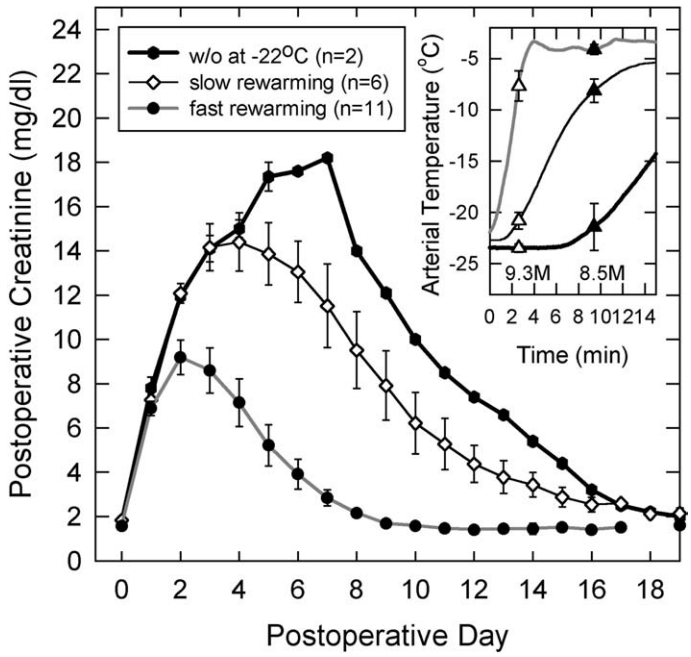

Fig. 8. Postoperative creatinine levels resulting from different methods of removing M22. At the end of the nominal M22 loading period (time zero in inset), appropriate valves were switched to begin dilution of M22 with VMP. At the same time, the temperature of the arterial heat exchanger began to be changed at one of three different rates. The inset shows the three resulting arterial temperature vs. time histories and highlights the times and temperatures at which the measured arterial concentration first began to drop (indicated by the open triangles at 9.3 M cryoprotectant) and finally began to approach the concentration of VMP (indicated by the filled triangles designating the attainment of 8.5 M cryoprotectant). The line types in the protocol inset match the line types for the same groups in the main panel showing postoperative results. The M22 perfusion time in the −22 °C washout group was 15 min. For the slow warming washout protocol, four kidneys were perfused with M22 for 15 min and two were perfused for 20 min. For the fast warming washout protocol, one kidney was perfused with M22 for 15 min, four were perfused for 20 min, and six were perfused for 25 min. There was no apparent influence of M22 perfusion time on postoperative creatinine levels. For example, in the fast warming group, the 25-min kidneys actually averaged slightly lower mean creatinine levels than the 20-min kidneys on most postoperative days (data not shown; no significant differences between 20 and 25 min subgroups). All points show means ± 1 SEM.

Cooling kidneys to below −40 °C

In order to develop procedures for cooling kidneys removed from the perfusion machine and to probe the impact of chilling injury below −22 °C, several M22-perfused kidneys were placed in a −50 °C environment for 6 min and then rewarmed for 4 min and reperfused for M22 washout. Cooling was accomplished using a Linde BF1 air cooling unit in which liquid nitrogen was injected into a vigorously circulated air chamber as needed to attain the desired temperatures. Upon warming, dry ambient temperature nitrogen was bled into the chamber to maintain a positive pressure in the unit and therefore avoid the formation of frost from the entry of ambient air into the cold chamber. The total time spent from removal of the kidney from the perfusion machine to the beginning of reperfusion was about 11 min. Fig. 10 shows an example of the cooling and warming procedure used in these experiments and the resulting thermal profiles within one sample kidney obtained using a three-junction needle thermocouple inserted directly into the kidney. The direct intrarenal temperature measurements were in agreement with expectation and confirmed that all parts of the kidney were at least as cold as −40 to −50 °C at the end of cooling. Presumably, the more superficial cortex approached the environmental temperature of −50 to −55 °C.

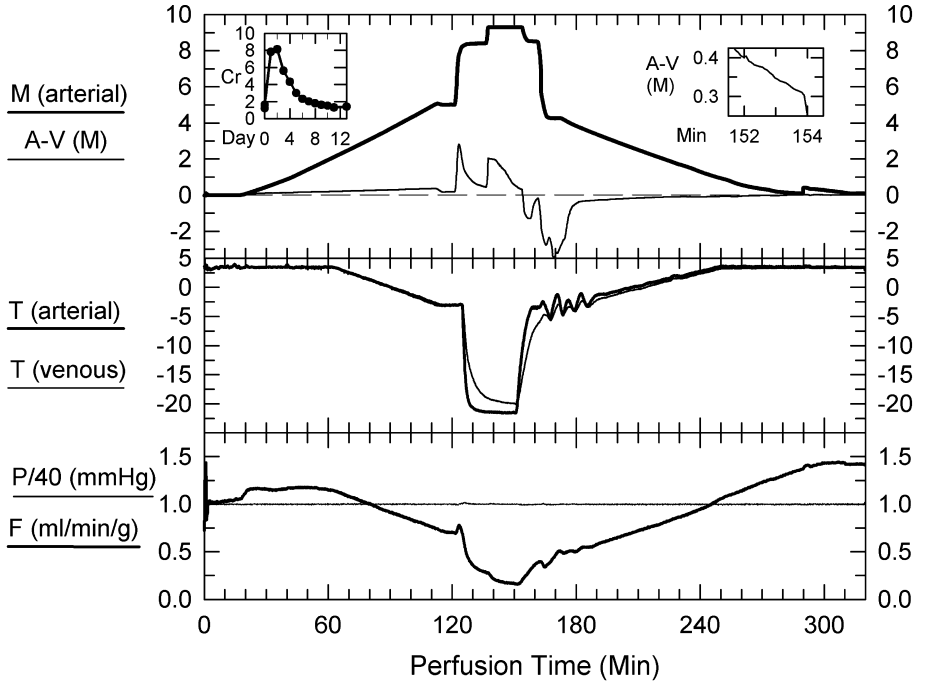

Fig. 9. Exemplary protocol for the successful recovery of kidneys after perfusion with M22 for 25 min at −22 °C. Format, abbreviations, and insets as in Fig. 7. The temperature control instabilities shown immediately after rapid warming from −22 °C were not typical of this protocol, but illustrate the tolerance of the kidney to mild temperature fluctuations within this range.

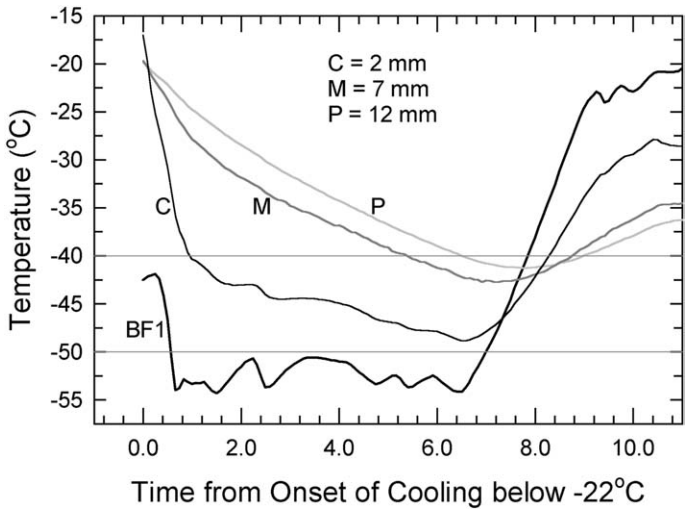

Fig. 10. Environmental and intrarenal thermal history of a rabbit kidney exposed to −50 °C by forced convection for 6 min and then rewarmed. C, cortical temperature (2 mm below the renal surface); M, medullary temperature (7 mm below the renal surface); P, papillary/pelvic temperature (12 mm below the renal surface); BF1, temperature of rapidly moving air in contact with the renal surface in a Linde BF-1 Biological Freezer. Intra-renal temperatures were monitored using a PhysiTemp (Huron, PA) triple bead needle probe. Horizontal lines illustrate that all parts of the kidney were between −40 and −50 °C at the time of onset of warming.

The average intrarenal temperature of ~−45 °C was about halfway between 0 °C and the ~−85 °C lower temperature limit for the augmentation of chilling injury according to Fig. 4, and is below the −40 °C found by Khirabadi et al. [30] to produce maximum chilling injury in their hands.

Fig. 11 compares the damage done by cooling to below −40 °C to the effects of simply perfusing M22 for different times according to the protocol of Fig. 9. All (8/8) kidneys recovered from ~−45 °C survived, but postoperative creatinine levels were elevated. However, the extra injury seen as a result of the 11-min process of cooling to and warming from −45 °C closely approximated the effect of perfusing M22 for an additional 5 min at −22 °C. It is therefore possible that some or all of the additional damage in the −45 °C kidneys could be related to the longer total exposure time rather than to chilling injury itself. Further, although the venous thermal profiles of these kidneys during reperfusion with −3 °C VMP were similar to those obtained for the control kidneys perfused at −22 °C without additional cooling (Fig. 12A), deep intrarenal temperatures at the

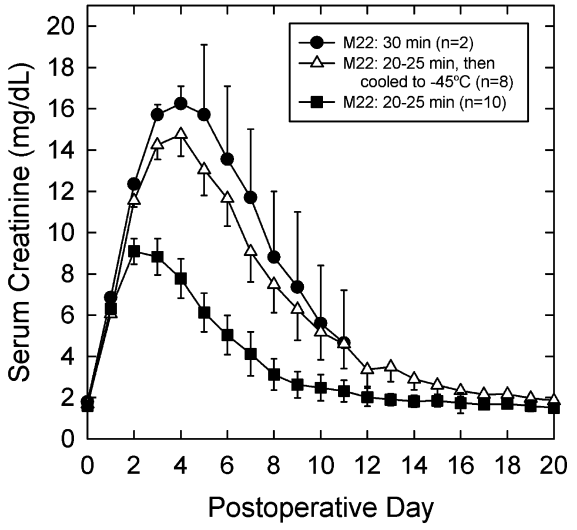

Fig. 11. Comparison of damage produced by perfusing M22 for different times at ~−22 °C according to the protocol of Fig. 9 or by cooling to ~−45 °C after perfusion with M22 at −22 °C. The 20–25 min M22 perfusion group included four 20-min perfusions and six 25-min perfusions. This is the same data set as in Fig. 8, but without the 15 min perfusion. The −45 °C group was perfused with M22 for 20 ($n = 2$) or 25 ($n = 6$) min before cooling and warming according to the protocol shown in Fig. 10. Means ± 1 SEM.

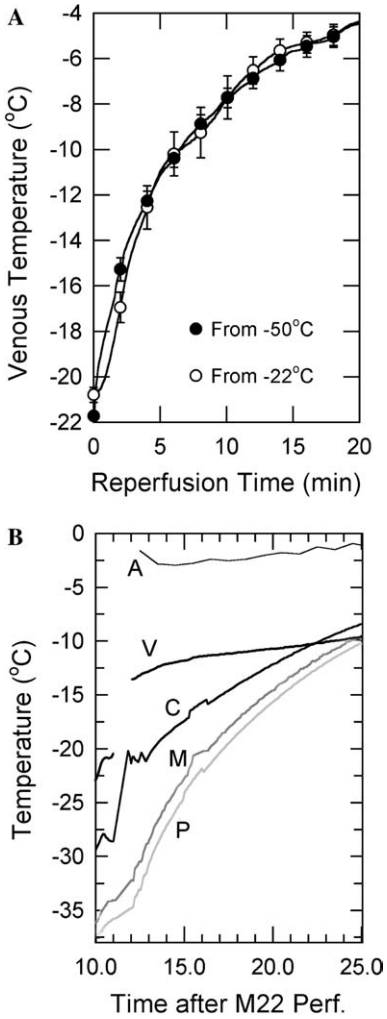

Fig. 12. (A) Venous temperatures during the reperfusion of kidneys after exposure to either −22 °C (white circles) or −45 °C (environment, ~−50 °C; black circles). (B) Vascular (arterial (A), venous (V)) and intrarenal (C, cortex; M, medulla; P, papilla/pelvis) thermal profiles during reperfusion of one kidney after previous exposure to ~−50 °C. The time axis indicates time since the end of M22 perfusion, 10 min being the time during which cooling and warming in the BF1 took place (see Fig. 10). The BF1 air temperature during rewarming but prior to reperfusion is indicated by the unlabeled line near the left axis of the graph. Reperfusion took place shortly before the beginning of the venous temperature trace. Note the low temperatures within the medulla and pelvis at the onset of reperfusion.

onset of reperfusion with VMP approximated −35 °C (Fig. 12B), which could put these areas at additional risk of osmotic expansion damage. The origin of the extra injury seen at −45 °C is important. If it reflects primarily an exacerbation of chilling injury, its further accumulation between −45 and −85 °C could well become overwhelming, but if it reflects injury from increased exposure time and/or osmotic expansion damage, then further cooling to −85 °C and below may have relatively little additional effect. Only more research will be able to address these key questions.

Evaluating susceptibility to devitrification

Another key question pertaining to the feasibility of attempting vitrification of the whole kidney is whether different renal subregions within perfused kidneys equilibrate with M22 sufficiently to remain unfrozen during both cooling to and warming from below T_g. To investigate this issue, kidneys were perfused with M22 according to the protocol of Fig. 9, then removed from the perfusion machine and longitudinally bisected. The exposed surfaces of the cortex, outer medulla, inner medulla, papilla, and pelvic tissue were biopsied and the biopsies were immediately placed into aluminum DSC pans and the pans were sealed. The samples were either evaluated immediately, or they were stored at −20 or at −128 °C until analyzed. The bisected kidneys were placed in thin plastic weighing tubs with or without immersion in M22 and placed into a Harris CryoStar freezer at −128 °C and allowed to cool passively in this way to below T_g (∼−124 °C) for later visual inspection for signs of ice. Fig. 13 shows the appearance of one such bisected rabbit kidney cooled without immersion and examined weeks after being placed into the freezer. Although the cortex, medulla, and papilla appear vitreous, the pelvic contents are bright white, suggesting freezing. Biopsy sites for DSC studies are visible in both hemikidneys.

Fig. 14 presents our first preliminary data on the stability of renal tissue biopsies against ice formation after rapid cooling to −150 °C and subsequent warming at 20 °C/min in a DSC. Although the cortex may be adequately protected from devitrification after perfusion times as short as 20 min, ice formation occurs during the warming of inner medullary and pelvic tissue even after 25 min of perfusion. Translated into the approximate mass fraction of the tissue that is converted into ice during cooling and warming in these specimens, just under 2% of the inner medulla and

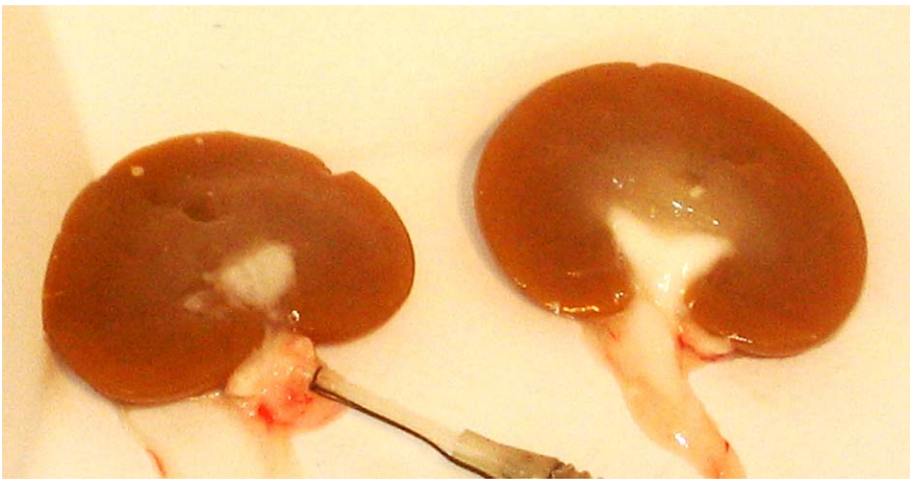

Fig. 13. Confinement of ice formation to the pelvis of a rabbit kidney that was perfused with M22 at −22 °C for 25 min, bisected, and allowed to passively cool in air in a CryoStar freezer at about −130 °C. White spots in cortex (left hemikidney) are contaminants, not ice. Cavities in medulla and cortex are sites of renal biopsies taken for DSC analysis of tissue cryoprotectant concentration and stability against ice formation; some white pelvis is visible through an inner medullary biopsy site in the right hemikidney. The vast majority of the kidney appears to have vitrified and is indistinguishable from the appearance of the kidney prior to cooling.

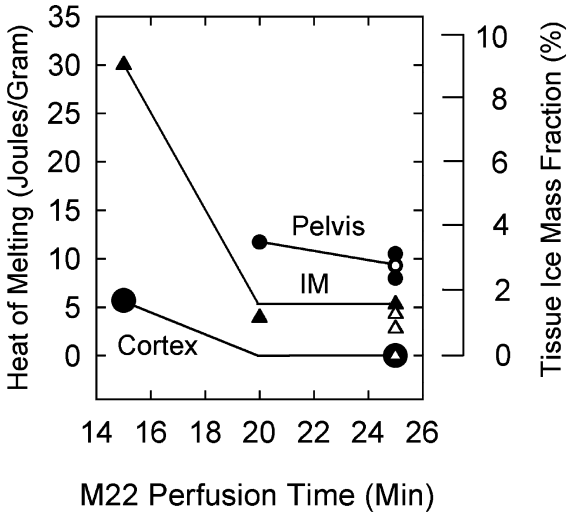

Fig. 14. Effect of M22 perfusion time and perfusion pressure on the amount of ice formed in rabbit renal subregions collected after whole kidney perfusion and cooled to −150 °C at 100 °C/min and rewarmed at 20 °C/min. Left axis: Joules of heat required per gram of sample to complete melting. Right axis: Heat of melting expressed as the percentage of sample mass that would be required to crystallize as ice in order to account for the enthalpies of melting given by reading the left axis. Percent of sample mass crystallized was calculated by dividing the melting enthalpies in J/g by 3.34 J/10 mg of ice melted (10 mg/g = 1% of the sample mass). Small circles: pelvic tissue biopsies. Triangles: inner medullary (IM) biopsies. Large circles: cortical biopsies. Black symbols: biopsies taken from kidneys perfused at 40 mmHg. White symbols: biopsies taken after perfusion at 60–100 mmHg.

somewhat under 4% of the pelvic tissue mass crystallizes, based on the size of the observed melts. Whether devitrification of this magnitude is damaging to these tissues remains to be determined. Elevating perfusion pressure from 40 to 60 or 100 mmHg seems to improve tissue stability somewhat (white symbols), but the effect is not dramatic or consistent, and the hazards of such perfusion pressures could of course obviate any gains attained.

These experiments provided not only heats of melting but also tissue melting points, as listed in Table 4. These melting points were converted into estimated tissue concentrations of M22 as follows. First, the melting points of various dilutions of M22 in LM5 were measured and assembled into a T_m curve for M22 (Fig. 15, circles). The data points were next fit with a cubic least squares regression line to enable accurate interpolation of the T_m curve over the range covered by the experimental points. Finally, putative tissue M22 concentrations were inferred as being those concentrations necessary to account for the observed tissue melting points based on the T_m curve fit (diamonds, Fig. 15). The resulting tissue concentrations are given in Table 4.

Examination of the data in Table 4 indicates that increasing perfusion time improves tissue M22 concentrations from about 84–90% of M22 at 15 min to about 87–>94% at 25 min. Comparing the amounts of ice formed and the glass transition temperatures in tissue biopsies versus various M22 dilutions (see lower section of Table 4 for data on diluted M22) indicates that tissues of a given melting point are more unstable than M22 dilutions of the same melting point. Nevertheless, the amount of ice formed in tissue samples taken after at least 20 min of perfusion is generally comparable to the amount of ice formed in M22 diluted to 90% of its full concentration, and warming the latter at 40 °C/min virtually abolishes its devitrification. It therefore seems possible that mild electromagnetic rewarming, improved equilibration, an ability to withstand a certain amount of ice formation, or some combination of these factors might allow kidneys to avoid fatal devitrification injury in future experiments, particularly if the freezing of pelvic tissue is innocuous. The last two columns of Table 4 compare tissue and venous cryoprotectant concentrations to determine how well the non-invasive measurement of effluent concentration can predict tissue concentrations determined by invasive sampling. It appears that the venous cryoprotectant concentration is a reasonably good indicator of the concentration of cryoprotectant in the inner medulla after different times of perfusion, although it may underestimate tissue concentrations at higher perfusion pressures.

It is probably not coincidental that the size of the deficit in tissue cryoprotectant concentration mirrors the relative perfusion rates of different renal regions in vivo. Under physiological conditions the cortex receives about 90% of renal blood flow, the outer medulla receives about 10%, and only 1–2% reaches the inner medulla and papilla [39]. Given

Table 4
Estimated renal tissue cryoprotectant concentrations after M22 perfusion[a]

M22 perfusion time (min)	Perfusion pressure	Tissue sampled	Tissue ΔH_M	Tissue T_g	Tissue T_m	Tissue M22 (% w/v)	Tissue % equilibration	Venous % equilibration	$100\% \times C_{Tiss}/C_{Ven}$
15	40	Cortex	5.7	−122.0	−42.0	58.25	89.9	84.7	106.1
15	40	IM[b]	30.0	−122.3	−36.7	54.7	84.4	84.7[b]	99.6
20	40	IM	3.9	−121.9	−39.9	56.9	87.8	93.6	93.8
25	40	Cortex	0.0	−118.6	nf[c]	—	—	97.9	—
			0.0(10)	−120.1(10)[d,e]	nf				
25	40	OM[b]	29.4	−122.6	−39.3	56.5	87.2	97.9[b]	89.1
25	40	IM[b]	5.3	−121.6	−42.9	58.85	90.8	97.9[b]	92.7
			10.2(10)[e]	−123.3(10)[e]	−44.5(10)[e]				
25	60	IM	2.8	−120.3	−45.9	60.7	93.7	96.7	96.9
25	100	IM	3.7(5)	−123.6(5)	−48.0(5)	60.9	94.0	97.5	96.4
25	100	IM	4.3	−121.6	−41.6	58.0	89.5	95.9	93.3
85% v/v M22 in LM5			21.8	−122.0	−37.7	55.1	(85.0)		
					−39.3(2)				
90% v/v M22 in LM5			0.14(40)	−118.7(40)	−38.7(40)				
			3.14	−120.6	−41.0	58.3	(90.0)		
					−44.2(2)				
94% v/v M22 in LM5			0.344	−119.6	−45.9	60.9	(94.0)		
			0.641(5)	−122.7(5)	−47.1(5)				
97% v/v M22 in LM5			0.00	−118.6	−50.6[f]	62.9	(97.0)		
			0.00(2)	−123.8(2)	nf				
			2.57(1)	−125.5(1)	−52.0(1)				
100% v/v M22 in LM5			nf	−123.3(2)	nf	64.8	(100.0)		

[a] *Explanation of column headings:* M22 perfusion time, programmed duration of M22 perfusion; perfusion pressure, arterial pressure, in mmHg; tissue sampled, renal subregion removed from the perfused kidney for DSC analysis (OM, outer medulla; IM, inner medulla); tissue ΔH_M, heat (in J/g) required to melt all ice that previously formed in the tissue sample during both cooling and warming as measured at a warming rate of 20 °C/min unless otherwise indicated; tissue T_g, tissue glass transition temperature measured at a warming rate of 20 °C/min unless otherwise indicated; tissue T_m, tissue melting point measured during warming at 20 °C/min unless otherwise indicated; tissue M22, apparent tissue concentration of M22 solutes, in % w/v units, derived as described below and in the text; tissue % equilibration = 100% × (tissue M22)/64.8, where 64.8 is the total concentration of M22 in % w/v units; venous % equilibration, apparent venous (effluent) concentration of M22 solutes, expressed as a percentage of the concentration of M22; $100\% \times C_{Tiss}/C_{Ven}$, the apparent tissue subregion cryoprotectant concentration (C_{Tiss}) expressed as a percent of the apparent venous cryoprotectant concentration (C_{Ven}). Apparent tissue M22 concentrations were estimated by either of two methods. In the first method, tissue T_m values obtained at a warming rate of 20 °C/min ($T_m(20)$ values) were compared directly to a version of Fig. 15 in which T_m values for dilutions of M22 were obtained at the same warming rate. In the second method, Fig. 15, which was derived using a warming rate of 2 °C/min for greater absolute accuracy of T_m, was used to obtain tissue M22 concentrations as follows. First, 1.85 °C was subtracted from the tabulated tissue $T_m(20)$ values in order to correct $T_m(20)$ values to T_m values expected at 2 °C/min. (1.85 °C is the mean difference in T_m values at the two warming rates for the examples shown in the table for various dilutions of M22.) Second, the value of % w/v M22 solutes having the same T_m as the corrected tissue T_m was read from inspection of Fig. 15. The results obtained using these two methods were virtually identical. *Note.* Numbers appearing in the bottom half of this table represent results for dilutions of M22, not for tissue samples.

[b] Same kidney as in the previous line in the table.

[c] nf = not freezable (unable to detect a melting point or a heat of melting under the conditions tested).

[d] Numbers in parentheses refer to the warming rate used when the warming rate employed to obtain a given measurement differed from 20 °C/min. For example, the T_g entry of "−123.3(10)" refers to the T_g in °C as measured during warming at 10 °C/min.

[e] Same tissue sample as in the previous line in the table.

[f] Melting point obtained by interrupting warming near −80 °C and allowing 1 h for ice growth prior to melting the sample at 20 °C/min.

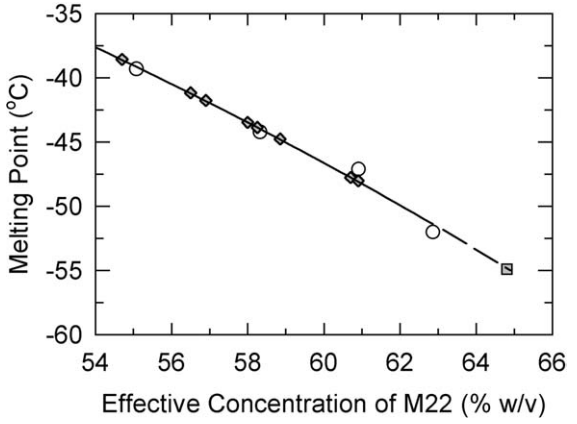

Fig. 15. Melting points (T_m curve, open circles) determined at a warming rate of 2 °C/min for various dilutions of M22 in LM5. Concentration is expressed as percent w/v, with M22 at 64.8% w/v. A theoretical melting point of M22 was obtained by extrapolation (square) since this solution could not be made to freeze under any conditions tested. Line: cubic polynomial fit through the open points and approximate "anchoring" points at (20% w/v, −7 °C) and (0% w/v, −0.5 °C). Diamonds: corrected melting points of tissue biopsies from Table 4, positioned at the apparent tissue concentrations necessary for them to fall on the T_m curve fit.

this, it is remarkable that the medulla and pelvis equilibrate as well as they do. The alternative hypothesis for reduced equilibration in these regions, which is lower membrane permeability to permeating cryoprotectants, seems unlikely in view of the fact that tissue exposed to fully impermeable osmolytes at the concentration of M22 should not only vitrify but should do so at high temperatures as intracellular proteins are concentrated by exosmosis [16] to as high as ~80% w/w [48]. Generally, if vitrifiable concentrations of cryoprotectant equilibrate osmotically with a given tissue, that tissue should vitrify whether the cryoprotectant actually enters the tissue and its cells or not.

Conclusions

Significant advances have been made in the fundamental cryobiology underlying the possibility of successful cryopreservation of organs by vitrification, and substantial progress has been made in applying these fundamental advances toward the vitrification of the rabbit kidney. Areas that require better definition include the significance of chilling injury below about −45 °C, the significance of crystallization of 1–4% of tissue mass, the efficacy and hazards of elevated perfusion pressures and other techniques for more rapidly distributing cryoprotectant to weakly circulated tissues, and the efficacy and hazards of electromagnetic warming methods. The ability to consistently recover kidneys after cooling to core temperatures of about −45 °C with subsequent long-term life support function after transplantation constitutes a previously unattainable milestone and provides the strongest evidence to date that the successful vitrification of whole organs may be achievable. Although the remaining barriers are significant, the conditions required for successful cryopreservation are not far different from those that can now be tolerated, and we have never been better informed about the obstacles that lie ahead.

Acknowledgments

Ms. Perlie Tam and Mr. David Ta provided skillful support as non-sterile surgical team members and phlebotomists, and Mr. Richard Infante provided essential support to our vivarium as well as occasional surgical services. This research was supported entirely by 21st Century Medicine, Inc. Because much of the material presented in this paper is the subject of pending or issued patents in various jurisdictions we encourage investigators to contact Mr. J. Dean Barry (jdbarry@21cm.com; 1-909-466-8633) to inquire about desired uses of the material.

References

[1] C.G. Adem, J.B. Harness, Computer control of a modified Langendorff perfusion apparatus for organ preservation using cryoprotective agents, Journal of Biomedical Engineering 3 (1981) 134–139.
[2] Anon., Cryopreservation of embryos, Lancet 1 (1985) 678.
[3] F.G. Arnaud, B. Khirabadi, G.M. Fahy, Physiological evaluation of a rabbit kidney perfused with VS41A, Cryobiology 46 (2003) 289–294.

[4] P. Boutron, P. Mehl, Theoretical prediction of devitrification tendency: determination of critical warming rates without using finite expansions, Cryobiology 27 (1990) 359–377.
[5] G.M. Fahy, Analysis of solution effects injury: cooling rate dependence of the functional and morphological sequellae of freezing in rabbit renal cortex protected with dimethyl sulfoxide, Cryobiology 18 (1981) 550–570.
[6] G.M. Fahy, Cryoprotectant toxicity: biochemical or osmotic?, Cryo-Letters 5 (1984) 79–90.
[7] G.M. Fahy, Biological effects of vitrification and devitrification, in: D.E. Pegg, A.M. Karow Jr. (Eds.), The Biophysics of Organ Cryopreservation, Plenum Press, New York, 1987, pp. 265–293.
[8] G.M. Fahy, Vitrification as an approach to organ cryopreservation: past, present, and future, in: C.T. Smit Sibinga, P.C. Das, H.T. Meryman (Eds.), Cryopreservation and Low Temperature Biology in Blood Transfusion, Kluwer, Boston, 1990, pp. 255–268.
[9] G.M. Fahy, An advantageous carrier solution for vitrifiable concentrations of cryoprotectants, and compatible cryoprotectant mixtures, United States Patent Application 09/916,396, 2001.
[10] G.M. Fahy, Hypertonic reduction of chilling injury, United States Patent Application Publication US 2002/0042042 A1, 2001.
[11] G.M. Fahy, S.E. Ali, Cryopreservation of the mammalian kidney. II. Demonstration of immediate ex vivo function after introduction and removal of 7.5 M cryoprotectant, Cryobiology 35 (1997) 114–131.
[12] G.M. Fahy et al., Cellular injury associated with organ cryopreservation: chemical toxicity and cooling injury, in: J.J. Lemasters, C. Oliver (Eds.), Cell Biology of Trauma, CRC Press, Boca Raton, 1995, pp. 11–22.
[13] G.M. Fahy, A. Hirsh, Prospects for organ preservation by vitrification, in: N.A. Halasz (Ed.), Organ Preservation, Basic and Applied Aspects, MTP Press, Lancaster, 1982, pp. 399–404.
[14] G.M. Fahy, D.I. Levy, S.E. Ali, Some emerging principles underlying the physical properties, biological actions, and utility of vitrification solutions, Cryobiology 24 (1987) 196–213.
[15] G.M. Fahy et al., Cryoprotectant toxicity and cryoprotectant toxicity reduction: in search of molecular mechanisms, Cryobiology 27 (1990) 247–268.
[16] G.M. Fahy et al., Vitrification as an approach to cryopreservation, Cryobiology 21 (1984) 407–426.
[17] G.M. Fahy, B. Wowk, Cryoprotectant solution containing dimethyl sulfoxide, an amide and ethylene glycol, United States Patent 6,395,467 B1, 2002.
[18] G.M. Fahy et al., Improved vitrification solutions based on predictability of vitrification solution toxicity, Cryobiology 48 (2004) 22–35.
[19] J. Farrant, Mechanism of cell damage during freezing and thawing and its prevention, Nature 205 (1965) 1284–1287.
[20] Z. Gavish, A. Arav, Survival of ovarian blood vessels after whole organ cryopreservation, Cryobiology 47 (2003) 264–265.
[21] R. Hamilton, H.I. Holst, H.B. Lehr, Successful preservation of canine small intestine by freezing, Journal of Surgical Research 14 (1973) 313–318.
[22] C.E. Huggins, Preservation of organized tissues by freezing, Federation Proceedings (Suppl. 15) (1965) S190–S195.
[23] C.J. Hunt, Studies on cellular structure and ice location in frozen organs and tissues: the use of freeze-substitution and related techniques, Cryobiology 21 (1984) 385–402.
[24] I.A. Jacobsen et al., Introduction and removal of cryoprotective agents with rabbit kidneys: assessment by transplantation, Cryobiology 25 (1988) 285–299.
[25] I.A. Jacobsen et al., Transplantation of rabbit kidneys perfused with glycerol solutions at 10 °C, Cryobiology 15 (1978) 18–26.
[26] J.O. Karlsson, M. Toner, Cryopreservation, in: R.P. Lanza, R. Langer, J. Vacanti (Eds.), Principles of Tissue Engineering, second ed., Academic Press, San Diego, 2000, pp. 293–307.
[27] A.M. Karow Jr., The organ bank concept, in: A.M. Karow Jr., G.J.M. Abouna, A.L. Humphries Jr. (Eds.), Organ Preservation for Transplantation, Little, Brown and Company, Boston, 1974, pp. 3–8.
[28] A.M. Karow Jr., M. Shlafer, Ultrastructure–function correlative studies for cardiac cryopreservation. IV. Prethaw ultrastructure of myocardium cooled slowly ($\leqslant 2$ °C/min) or rapidly ($\geqslant 70$ °C/s) with or without dimethyl sulfoxide (DMSO), Cryobiology 12 (1975) 130–143.
[29] B. Khirabadi, G.M. Fahy, Permanent life support by kidneys perfused with a vitrifiable (7.5 molar) cryoprotectant solution, Transplantation 70 (1) (2000) 51–57.
[30] B.S. Khirabadi, F. Arnaud, E. Kapnik, The effect of vitrification on viability of rabbit renal tissue, Cryobiology 37 (1998) 447.
[31] B.S. Khirabadi et al., 100% survival of rabbit kidneys chilled to −32 °C after perfusion with 8 M cryoprotectant at −22 °C, Cryobiology 31 (1994) 597.
[32] B.S. Khirabadi, G.M. Fahy, L.S. Ewing, Survival of rabbit kidneys perfused with 8.4 M cryoprotectant, Cryobiology 32 (1995) 543–544.
[33] B.S. Khirabadi et al., Failure of rabbit kidneys to survive chilling to −30 °C after perfusion with 8 M cryoprotectant at −3 °C, Cryobiology 31 (1994) 596–597.
[34] B.S. Khirabadi et al., Life support function of rabbit kidneys exposed to extreme hydrostatic pressure, Cryobiology 29 (1992) 722.
[35] B. Luyet, On the amount of water remaining amorphous in frozen aqueous solutions, Biodynamica 10 (1969) 277–291.
[36] B. Luyet, D. Rasmussen, Study by differential thermal analysis of the temperatures of instability of rapidly cooled solutions of glycerol, ethylene glycol, sucrose, and glucose, Biodynamica 10 (1968) 167–191.
[37] M.J. Lysaght, N.A. Nguy, K. Sullivan, An economic survey of the emerging tissue engineering industry, Tissue Engineering 4 (3) (1998) 231–238.

[38] P. Mehl, Nucleation and crystal growth in a vitrification solution tested for organ cryopreservation by vitrification, Cryobiology 30 (1993) 509–518.
[39] J. Ofstad, K. Aukland, Renal circulation, in: D.W. Seldin, G. Giebisch (Eds.), The Kidney, Physiology and Pathophysiology, Raven Press, New York, 1985, pp. 471–496.
[40] D.E. Pegg, Banking of cells, tissues, and organs at low temperatures, in: A.U. Smith (Ed.), Current Trends in Cryobiology, Plenum Press, New York, 1970, pp. 153–180.
[41] D.E. Pegg, Theory and experiments towards subzero organ preservation, in: D.E. Pegg (Ed.), Organ Preservation, Churchill Livingstone, London, 1973, pp. 108–122.
[42] D.E. Pegg, Perfusion of rabbit kidneys with glycerol solutions at 5 °C, Cryobiology 14 (1977) 168–178.
[43] D.E. Pegg, Ice crystals in tissues and organs, in: D.E. Pegg, A.M. Karow Jr. (Eds.), The Biophysics of Organ Cryopreservation, Plenum, New York, 1987, pp. 117–140.
[44] D.E. Pegg, M.P. Diaper, The mechanism of cryoinjury in glycerol-treated rabbit kidneys, in: D.E. Pegg, I.A. Jacobsen, N.A. Halasz (Eds.), Organ Preservation, Basic and Applied Aspects, MTP Press, Lancaster, 1982, pp. 389–393.
[45] C. Polge, A.U. Smith, A.S. Parkes, Revival of spermatozoa after vitrification and dehydration at low temperatures, Nature 164 (1949) 666.
[46] W.F. Rall, G.M. Fahy, Ice-free cryopreservation of mouse embryos at −196 °C by vitrification, Nature 313 (1985) 573–575.
[47] G. Rapatz, R. Keener, Effect of concentration of ethylene glycol on the recovery of frog hearts after freezing to low temperatures, Cryobiology 11 (1974) 571–572.
[48] D. Rasmussen, B. Luyet, Contribution to the establishment of the temperature–concentration curves of homogeneous nucleation in solutions of some cryoprotective agents, Biodynamica 11 (1970) 33–44.
[49] G.J. Sherwood, J.R. Flower, Engineering aspects of equipment design for subzero organ preservation, in: D.E. Pegg (Ed.), Organ Preservation, Churchill Livingstone, London, 1973, pp. 152–174.
[50] A.U. Smith, Problems in the resuscitation of mammals from body temperatures below 0 °C, Proceedings of the Royal Society Series B 147 (1957) 533–544.
[51] A.U. Smith, Biological Effects of Freezing and Supercooling, Edward Arnold, London, 1961.
[52] A.U. Smith, The effects of glycerol and of freezing on mammalian organs, in: A.U. Smith (Ed.), Biological Effects of Freezing and Supercooling, Edward Arnold, London, 1961, pp. 247–269.
[53] Y.C. Song et al., In vivo evaluation of the effects of a new ice-free cryopreservation process on autologous vascular grafts, Journal of Investigative Surgery 13 (2000) 279–288.
[54] Y.C. Song et al., Vitreous cryopreservation maintains the function of vascular grafts, Nature Biotechnology 18 (2000) 296–299.
[55] T.E. Starzl, A look ahead at transplantation, Journal of Surgical Research 10 (1970) 291–297.
[56] T. Takahashi, R.J. Williams, Thermal shock hemolysis in human red cells. I. The effects of temperature, time, and osmotic stress, Cryobiology 20 (1983) 507–520.
[57] X. Wang et al., Fertility after intact ovary transplantation, Nature 415 (385) (2002).
[58] B. Wowk, G.M. Fahy, Inhibition of bacterial ice nucleation by polyglycerol polymers, Cryobiology 44 (2002) 14–23.
[59] B. Wowk et al., Vitrification enhancement by synthetic ice blocking agents, Cryobiology 40 (2000) 228–236.